*Article*

# Modern Pyromes: Biogeographical Patterns of Fire Characteristics across the Contiguous United States

Megan E. Cattau [1,*], Adam L. Mahood [2,3], Jennifer K. Balch [2,4] and Carol A. Wessman [2,5]

[1] Human-Environment Systems, Boise State University, Boise, ID 83706, USA
[2] Earth Laboratory, Cooperative Institute for Research in Environmental Sciences (CIRES), University of Colorado, Boulder, CO 80303, USA; adam.mahood@colorado.edu (A.L.M.); jennifer.balch@colorado.edu (J.K.B.); carol.wessman@colorado.edu (C.A.W.)
[3] USDA Agricultural Research Service, Fort Collins, CO 80526, USA
[4] Department of Geography, University of Colorado, Boulder, CO 80309, USA
[5] Ecology and Evolutionary Biology & Environmental Studies, University of Colorado, Boulder, CO 80309, USA
[*] Correspondence: megancattau@boisestate.edu

**Abstract:** In recent decades, wildfires in many areas of the United States (U.S.) have become larger and more frequent with increasing anthropogenic pressure, including interactions between climate, land-use change, and human ignitions. We aimed to characterize the spatiotemporal patterns of contemporary fire characteristics across the contiguous United States (CONUS). We derived fire variables based on frequency, fire radiative power (FRP), event size, burned area, and season length from satellite-derived fire products and a government records database on a 50 km grid (1984–2020). We used k-means clustering to create a hierarchical classification scheme of areas with relatively homogeneous fire characteristics, or modern 'pyromes,' and report on the model with eight major pyromes. Human ignition pressure provides a key explanation for the East-West patterns of fire characteristics. Human-dominated pyromes (85% mean anthropogenic ignitions), with moderate fire size, area burned, and intensity, covered 59% of CONUS, primarily in the East and East Central. Physically dominated pyromes (47% mean anthropogenic ignitions) characterized by relatively large (average 439 mean annual ha per 50 km pixel) and intense (average 75 mean annual megawatts/pixel) fires occurred in 14% of CONUS, primarily in the West and West Central. The percent of anthropogenic ignitions increased over time in all pyromes (0.5–1.7% annually). Higher fire frequency was related to smaller events and lower FRP, and these relationships were moderated by vegetation, climate, and ignition type. Notably, a spatial mismatch between our derived modern pyromes and both ecoregions and historical fire regimes suggests other major drivers for modern U.S. fire patterns than vegetation-based classification systems. This effort to delineate modern U.S. pyromes based on fire observations provides a national-scale framework of contemporary fire regions and may help elucidate patterns of change in an uncertain future.

**Keywords:** anthropogenic ignitions; disturbance ecology; extremes; machine learning; satellite data; wildfire

## 1. Introduction

Human activity has influenced wildfire across the globe in recent millennia, either by increasing or suppressing fire activity. Although climate is widely recognized as a primary driver of fire activity globally [1,2], human activities modify that relationship. In fact, human activities may even have a larger effect than climate on fire activity, both in modern and historical contexts [3–6].

In recent decades, the United States (U.S.) has experienced pressures from land-use conversion, invasive species, increasing ignitions, and a warming climate that, in combination, are changing contemporary fire patterns [7–12]. These changes have forced the question of what past, current, and future fire regimes look like. Completely 'natural' fire

regimes are likely non-existent in modern North America [13]. People both alter ignitions dynamics and influence the factors that predispose an area to burning. For example, 84% of ignitions in the U.S. between 1992 and 2013 were anthropogenic, contributing substantially to the spatial and temporal characteristics of wildfires nationally [8,9]. Further, the expansion of the wildland–urban interface through new housing development is poised to alter wildfire dynamics as more people are placed in proximity to potential fuel loads [14].

In general, fire regime concepts are a framework for evaluating the spatiotemporal patterns of fire. Fire regimes, primarily controlled by climate, fuel, and/or ignitions, are often defined by fire parameters. In a strict definition, fire regimes are described by fire physical characteristics in space and time (fire *sensu stricto*, e.g., fire size, duration, severity); a broader definition of fire regimes could include the conditions under which fire can occur (fire *sensu lato*, e.g., vegetation and climate conditions, etc.) or even the effects of fire on the larger landscape [15–17]. Fire regimes are dynamic and complex, as fire characteristics interact with one another, with landscape patterns, and with climate dynamics over space and time [18]. Comparing fire characteristics over space and time and with social and environmental correlates of fire can reveal the relative influence of factors driving and constraining fire characteristics, patterns of change, and predictions of risk to ecosystems or society.

Satellites have given the fire science community a new view, based on different sensors' ability to detect fire-caused thermal and spectral changes [19]. Combined with government records, using satellite data has expanded our ability to quantify fire at the U.S. scale, which has provided unique perspectives on fire activity, the drivers behind fire activity, and the impacts of fires on human and natural systems [7,8,20]. In particular, standardized, national-scale data on ignition type from U.S. government records have been generated in recent times with the Fire Program Analysis fire-occurrence database FPA-FOD [21], and these data have provided key insights into the anthropogenic influence on fire regimes [8,9,22]. Moreover, the fire regime concept was developed well before the advent of remote sensing [16], leaving an opportunity to explore how new metrics (e.g., fire radiative power) made possible by the integration of multiple satellite sources may contribute to the fire regime concept. Although there have been efforts to delineate pyromes globally using remote sensing data [23], these have not yet been fully resolved for the U.S. and do not emphasize extreme values.

Here, we use satellite-derived fire products and a government records database to define the spatiotemporal patterns of contemporary fire in CONUS. We (1) delineated modern U.S. 'pyromes,' or areas that shared relatively homogenous fire characteristics, (2) described these pyromes based on their fire characteristics and rates of change (i.e., *sensu stricto*), (3) identified how these pyromes co-occurred spatially with anthropogenic ignitions, vegetation type, and climate (i.e., *sensu lato*) and if they were consistent with a historical national-scale classification of fire regimes and contemporary ecosystem types, and (4) evaluated the constraints on fire that occurred in each pyrome. We used the term 'pyrome' rather than 'fire regime' to describe our delineated fire clusters. Defining modern fire regimes is complicated by the uncertainty surrounding current dynamic changes in fire characteristics; these changes may be reflective of distributional shifts in fire characteristics and indicative of longer-term trends, or they may be within the historical range of variation [18,24]. As we used contemporary fire data from an approximately 40-year period to delineate fire clusters, we use the term 'pyrome' to differentiate this effort from those that consider deeper historical data. This effort provides a national-scale framework and map of modern U.S. 'pyromes' that is a complimentary addition to other national-scale databases on fire regimes and drivers, e.g., [25].

## 2. Materials and Methods

### 2.1. Fire Data and Preprocessing

We used publicly available fire products to calculate fire characteristics for CONUS, including the Moderate Resolution Imaging Spectroradiometer (MODIS) Active Fire Prod-

uct [26] 2003–2020, Monitoring Trends in Burn Severity (MTBS) Burned Areas Boundaries Dataset [27] 1984–2020, and the Fire Program Analysis fire-occurrence database (FPA-FOD) [28] 1992–2018. The MODIS dataset was used to calculate fire frequency, fire radiative power (FRP), and fire season length. The dataset includes all fires detected by either the Terra or Aqua MODIS sensor at the time of satellite overpass based on the mid-infrared radiation of the fire, and the fire detections are not grouped into fire events. The MTBS dataset was used to calculate fire frequency, fire event size, burned area, and fire season length. The dataset includes fire events over a size threshold (Western U.S., c. 405 hectares (ha); Eastern U.S., c. 202 ha) delineated manually by the MTBS project using a Landsat satellite-derived fire index. The FPA-FOD dataset was used to calculate fire frequency, fire event size, burned area, fire season length, and ignition type. It includes fire events based upon wildfire records from federal, state, and local fire organization reports.

Each dataset captures fires, and thus fire statistics, differently. For example, MODIS-based fire frequency captures the number of fire detections rather than fire events; while MTBS- and FPA-FOD-based fire frequency captures fire events. FPA-FOD includes fire events independent of size but only those that required a suppression response, while MTBS captures only large fires and includes both wildland and prescribed fires. MODIS includes all wildfires or prescribed fires that can be detected, though statistical error exists as a function of environmental factors (e.g., varying errors of commission and omission in different land-cover types) and data collection artifacts (e.g., view angle, resulting in a finer spatial resolution of pixels viewed from nadir relative to that of pixels located closer to the edge of the swath and thus a greater probability of detection of small fires at nadir) [29]. Some fire characteristics are only provided by one dataset. For example, FPA-FOD includes ignition type (e.g., 'lightning,' 'campfire,' 'arson'), which is the best available national-scale information regarding wildfire ignition source. MODIS includes FRP, which we used to represent 'FRP-based fire intensity.' FRP is the amount of energy released from the fire at the time of overpass and is related to combustion and fuel amount [30,31]. Although FRP is often considered a measure of fire intensity [32], it is important to note that FRP values will have systematic biases related to view angle and fire size, as FRP measurements are affected by both pixel size and the proportion of the pixel that the fire occupies. Although uncertainty in FRP related to view angle is reduced at coarse aggregations [33], particularly resolutions that capture all view angles, both off-nadir pixels and large fires would likely contribute disproportionately to aggregate FRP values. FRP-based intensity at coarse aggregations could be considered an indicator of fuel consumption.

Following Cattau et al. [9], we computed a suite of 15 fire characteristics derived from the information embedded in these aforementioned satellite sources and government records (Table 1 and Figure S1) by sampling these characteristics across a 50 km resolution grid at an annual temporal resolution across CONUS. We selected a resolution of 50 km since it is the approximate size of an average U.S. county to account for differences in the spatial resolution of the input fire datasets and because it is a sufficiently large aggregation to minimize data uncertainty related to view angle [33]. For each variable, we calculated the mean per grid cell per year to describe the average fire physical characteristics. We also calculated the maximum values for fire event size and FRP-based fire intensity to describe the most extreme fire physical characteristics. All variables were calculated contingent upon fire occurrence and otherwise assigned a value of zero. For all fire characteristics (e.g., fire event size) that were represented by multiple variables derived from different data sources, we ensured that these variables were not redundant. All had significantly different values ($p < 0.01$), determined by Wilcoxon rank-sum tests when there were two data sources and Kruskal–Wallis tests followed by pairwise Wilcoxon rank-sum tests when there were three data sources. More detail on data and data pre-processing—including more explanation of what is captured by each data source, justification for variable selection, and data caveats—is available in Cattau [9]. Unless otherwise noted, analyses were conducted using R version 4.2.0 [34].

**Table 1.** Fire characteristics derived for the contiguous U.S. at a 50 km spatial resolution and an annual temporal resolution (values are per pixel per year) from satellite data and government records to delineate modern pyromes based on fire physical characteristics. All data were derived from the Moderate Resolution Imaging Spectroradiometer (MODIS) Active Fire Product for 2003–2020, from the Monitoring Trends in Burn Severity (MTBS) Burned Areas Boundaries Dataset for 1984–2015, and from the Fire Program Analysis fire-occurrence database (FPA-FOD) for 1992–2015.

| Characteristic | | Data Source | Units |
|---|---|---|---|
| Fire frequency | | MODIS, MTBS, FPA-FOD | Total number of fires or fire detections (n) |
| Fire intensity | Average<br>Extreme | MODIS | Mean fire radiative power (FRP) (megawatts, MW)<br>Maximum FRP (MW) |
| Fire event size | Average<br>Extreme | MTBS, FPA-FOD | Mean area (hectares, ha)<br>Maximum area (ha) |
| Burned area | | MTBS, FPA-FOD | Sum area (ha) |
| Fire season length | | MODIS, MTBS, FPA-FOD | Standard deviation Julian Day (JD) multiplied by 2 |
| Ignition type | | FPA-FOD | Percent of fires ignited by humans (%) and percent of fires ignited by lightning (%) |

## 2.2. Variable Selection

We ran a principal components analysis (PCA) using the standardized and centered mean values for each variable to evaluate which fire variables accounted for most of the variance in the data and thus which variables to use to define the pyromes, and which fire variables were redundant or uninformative and thus could be excluded. Ignition type (i.e., human- or lightning-started) was not included because it is not a physical characteristic. The PCA realigned the data along new axes, or components, effectively reducing the dimensionality of the data by maximizing the variance captured by each component. We determined how many components to keep for further analysis (i.e., removed components which did not provide sufficient information) using the Kaiser criterion and by evaluating a scree plot. The Kaiser criterion suggests retaining those PCA components whose associated eigenvalue is greater than 1. We calculated eigenvalues using the R package 'factoextra' [35] (Table S1). We also visually evaluated a scree plot, in which the variance in the data was displayed as a function of the number of PCA components, to identify the number of components after which the amount of additional variance explained by retaining additional components was small (Figure S2). Any variables that were not significantly loaded on (i.e., were not correlated with) any of the remaining PCA components were excluded from the analysis (Figures S3 and S4 and Table S2).

## 2.3. Pyrome Delineation

We delineated the pyromes across a range of scales based on the fire characteristics. We used an unsupervised statistical learning method by employing a k-means clustering approach to identify unique groups of pixels that share similar fire characteristics. First, because the final number of clusters (i.e., pyromes) must be specified with this modeling approach but the ideal number of clusters was not known *a priori*, we started by estimating the maximum reasonable number of *k*. We ran 149 iterations of the algorithm with *k* values from 2–150 *k*, where *k* = the number of clusters. We determined the maximum number of clusters by computing the Bayesian information criterion (BIC) for each *k* and identified the value of *k* at which adding additional clusters increased the BIC (i.e., the threshold of *k* at which adding additional clusters no longer improved model fit; Figure S5).

Second, we determined how many clusters to retain for each level of the pyromes classification. We identified which values of *k* maximized between-cluster variation (i.e., separation) while minimizing within-cluster variation (i.e., compactness) by examining the Dunn index for each value of *k* using the R package 'clValid' [36]. The Dunn index is the ratio of the smallest inter-cluster distance in environmental space among observations (i.e.,

maximum compactness of clusters by fire characteristics) to the largest intra-cluster distance in environmental space (i.e., maximum separability of clusters by fire characteristics). We observed a set of possible $k$ and identified all $k$ which had the highest corresponding Dunn indices (i.e., local maxima across the set; Figure S6), which indicated the number of pyromes to be retained for each level.

*2.4. Pyrome Characterization*

We defined each modern pyrome *sensu stricto* by calculating the mean and standard deviation values for all fire physical characteristics by cluster. Fire characteristics were compared between pyromes pairwise using Tukey's post hoc test on one-way analysis of variance. Grid cells without fire were masked from the analysis for all variables except fire frequency. The rate of change for each fire characteristic for each pyrome group was estimated by partitioning the data into pyrome groups and fitting an individual linear model for each partition using the R package 'nlme' [37]. Pyrome groups were considered to have different rates of change from one another if they had non-overlapping confidence intervals.

Although these analyses were conducted for all fire characteristics and all results were reported in the Supporting Information (Table S3), we presented results for select variables throughout the main body of the article (Results section). We chose to present MODIS-based FRP because MODIS is the only data source that includes this information. Because we evaluated fire ignition type, which is information embedded in the FPA-FOD database (see below), we chose to present mean fire event size, frequency, burned area, and season length derived from FPA-FOD for consistency. Although satellite products (MTBS and MODIS) would not contain the human detection biases embedded in government records and thus differences in reporting among states and over time, we used the FPA-FOD for these analyses because the MTBS datasets include only fires over a size threshold (excluding many fires and affecting mean fire size, frequency, burned area, and perhaps season length) and MODIS does not group fire detections into fire events (affecting mean fire size, frequency, and burned area). Time series analysis using the FPA-FOD database were not spatially disaggregated by state to avoid spatial inconsistencies in reporting by state.

Modern pyromes were characterized *sensu lato* by the primary controls on fire—vegetation, climate, and ignition type—to identify how they mapped onto the contemporary spatial patterns of these controls. We calculated the percentage of each pyrome that was occupied by each category of the 2016 National Land Cover Database (NLCD) [38], temperature- and moisture-based climate zones (Koppen–Geiger climate classification) [39], and FPA-FOD ignition type. For the purposes of the ignition type characterization, a grid cell was considered dominated by anthropogenic or lightning ignitions if over 75% of ignitions in that grid cell were human or lightning-caused, respectively; otherwise, it was considered dominated by neither human nor lightning ignitions. Ignition cases that were unspecified or labeled as missing/unidentified (8.0% of all fires) were excluded from analyses related to ignition type.

Pyromes were also characterized by ecoregion (Environmental Protection Agency (EPA) Level 1 ecoregions) [40–43] and historical fire regime (LANDFIRE fire regime group (FRG)) [25]. The EPA ecoregions delineate areas that are ecologically similar in terms of the type and quality of environmental resources and are intended as a spatial framework for research and management. Characterizing our pyromes by the EPA ecoregions provided a way to compare our framework based on fire characteristics with a framework that includes a variety of ecological variables, including soils, land surface form, potential natural vegetation, land use, etc. The LANDFIRE FRG data characterize the presumed historical fire regime of an area (i.e., fire return interval (FRI) and severity) based on vegetation, fire spread and effects, and spatial context, thus providing a way to frame contemporary fire processes described in this paper within a historical context. We reported any class that constituted at least 20% of a

given pyrome for each category. A comprehensive description of each pyrome can be found in Appendix A: Description of the pyromes ($k = 8$).

### 2.5. Constraints on Fire

To explore the constraints on fire, or the trade-offs between fire physical characteristics in fire niche space, we plotted the multidimensional space that fire occupied for each pyrome, and we evaluated pairwise comparisons of characteristics for each pyrome.

## 3. Results
### 3.1. Variable Selection

Based on the Kaiser criterion and the scree plot, we retained the first four components of the PCA (Figure S2 and Table S1). All fire characteristics loaded significantly onto, i.e., were correlated with, at least one of these four components, and therefore we included all of these variables in further analyses (Figures S3 and S4 and Table S2). Thus, we used the entire suite of fire characteristics outlined in Table 1 except ignition type to inform the pyrome clustering algorithm.

### 3.2. Pyrome Delineation

The final, non-nested hierarchical pyromes classification scheme contained several levels with varying numbers of $k$ (i.e., pyromes) among levels. The maximum reasonable number of pyromes was identified as 39 pyromes (Figure S5). We found 12 levels of $k$ where the Dunn index reached local maxima: $k = 2, 5, 8, 14, 19, 24, 28, 30, 32, 35, 37,$ and 39 (Figure S6). These cut points in $k$ each represented a possible pyrome classification scheme, or level in the pyromes product. For example, at cut point $k = 8$, the resulting pyromes map displayed each 50 km resolution pixel classified as one of eight possible pyromes. Maps of all classification levels with local maxima Dunn indices are included in the Supporting Information (Figure S7).

Here, we focused on the third-level classification of the pyromes product, which contained eight major modern pyromes (Figure 1, disaggregated pyromes in Figure S8), although all levels mentioned above were valid (e.g., $k = 5$ and associated characteristics displayed in Figure S9). Evaluation of the Dunn indices indicated that $k = 8$ resulted in the best fit, or the highest Dunn index after $k = 2$, meaning the maximum within-cluster compactness and the maximum between-cluster separability. Further, as we were interested in comparing our modern pyromes to historical fire regime groups and in evaluating the heterogeneity of the controls of fire in each modern pyrome, we selected a $k$ among the established cut points of $k$ that would most easily allow us to make those comparisons. $K = 8$ was the most parsimonious with the other variables of interest (i.e., five historical fire regime groups, two categories of ignition type, five climate zones, and six terrestrial vegetation or land-cover types), though $k = 2, 5, 14, 19, 24, 28, 30, 32, 35, 37,$ and 39 were also valid classifications. The nestedness of pyromes at $k = 8$ with those at the other levels of classification are included in the Supporting Information (Figure S10). A depiction of the heterogeneity of pyromes at $k = 8$ (the level on which we focused) described by the characteristics of pyromes at $k = 39$ (the level with the most finely resolved pyromes) is included in the Supporting Information (Figure S11).

### 3.3. Pyrome Characterization

The human-dominated pyromes 3, 4, and 8 had the highest percent of pixels with human-dominated ignitions (78%, 69%, and 90%, respectively) (Figure 2). See Description of the pyromes ($k = 8$) in the Appendix A for a comprehensive description of each pyrome and Tables S3–S5 for details. Together, they occupied 59% of the land area of CONUS. Pyrome 3 occurred in the Northeast and North Central U.S. and had the highest rate of increase in anthropogenic fires over time: 1.7% ($\pm 0.03$) annual percent increase. Pyromes 4 and 8 occurred in the Southeast and South Central U.S. (in addition to some areas in central California), and both were distinguished by long season lengths: 167 ($+/-30.8$) and 173.6

(+/−29.6) mean annual days, respectively. Pyrome 4 was additionally characterized by high-frequency fire: 56.5 (+/−53.5) mean annual fires per pixel. Pyromes 3 and 8 were relatively spatially aggregated compared with pyrome 4. All had moderate fire size, burned area, and fire intensity (Table S3).

The physically dominated pyromes 1, 5, 6, and 7 had a low-to-moderate percent of pixels that were dominated by human ignitions (21%, 41%, 17%, and 0% of ignitions, respectively). They together occupied only 14% of the U.S. land area, almost exclusively distributed across the Western and West Central U.S., with pyrome 7 being confined to a relatively small cluster in the Great Plains. These pyromes exhibited the highest values of fire size, fire intensity, and burned area, both for average and extreme fires. For example, the highest mean annual intensity values occurred in pyromes 1 and 6, and the values for these pyromes were not significantly different from one another (nor were the values for pyrome 7) (Table S3). This was true for both average fires (mean FRP), for which pyrome 6 had the highest value (77.1 (+/−40.3) mean annual MW/pixel), and extreme fires (i.e., maximum FRP) for which pyrome 1 had the highest value (691.9 (+/−479.7) mean annual MW/pixel). Pyromes 1 and 6 both occurred in arid climates, with pyrome 1 occurring in shrubland and herbaceous areas and pyrome 6 in shrubland and forest areas. Whereas pyromes 1 and 6 were distinguished almost exclusively by their intensity, pyromes 5 and 7 were distinguished by their size. Pyrome 5 had the highest value of maximum (i.e., extreme) fire size and burned area, the fastest rate of increase for those variables, and the highest value of mean fire size according to MTBS. Pyrome 7 had the highest values for mean fire size, maximum fire size, and burned area, as well as rates of increase for those variables, according to FPA-FOD; it also had the highest rate of increase for mean fire size according to MTBS. Both pyromes also ranked high in values and/or trends for frequency and intensity. Whereas pyrome 5 was very mixed in terms of climate and land-cover type, pyrome 7 was much more homogeneous, occurring in temperate herbaceous areas. This homogeneity was due in part to the relatively small extent of pyrome 7. Falling more in the middle of the spectrum from human- to physically dominated, pyrome 2 occupied 27% of CONUS distributed across the Western and West Central U.S. This pyrome does not have the highest values for any of the fire characteristics assessed and relatively low human ignitions (24% of ignitions).

Except for pyrome 7 with a small spatial extent, no pyrome had the majority of its area occupied by any one land-cover type or historical fire regime (Tables S4 and S5). None except pyrome 7 had more than 63% of its area in a given ecoregion, though several did have the majority of their area in a given climate zone.

All pyromes had a significantly increasing percent of ignitions that were anthropogenic over time (0.5–1.7% of ignitions annually), though the slope for pyrome 7 was not significant. All pyromes except pyromes 1 and 7 had a significantly increasing fire frequency over time according to at least one dataset, and all pyromes except 7 did for season length. However, some significant negative slopes for fire frequency over time existed for pyromes 4, 6, and 8, and some significant negative slopes for season length over time existed only according to MTBS for pyromes 2, 3, 4, and 6. All pyromes except two (pyromes 3 and 8) had significantly increasing fire size and/or burned area according to at least one dataset (and no significant negative slopes). Trends in fire intensity were more mixed.

Results were not always consistent across datasets. For example, pyrome 5 had the largest mean and maximum fire size and burned area according to MTBS, and pyrome 7 did according to FPA-FOD. Similarly, pyrome 8 had the longest season length according to MODIS and FPA-FOD, but pyrome 4 did according to MTBS. Pyrome 4 had the highest fire frequency according to MTBS and FPA-FOD, and pyrome 5 did according to MODIS.
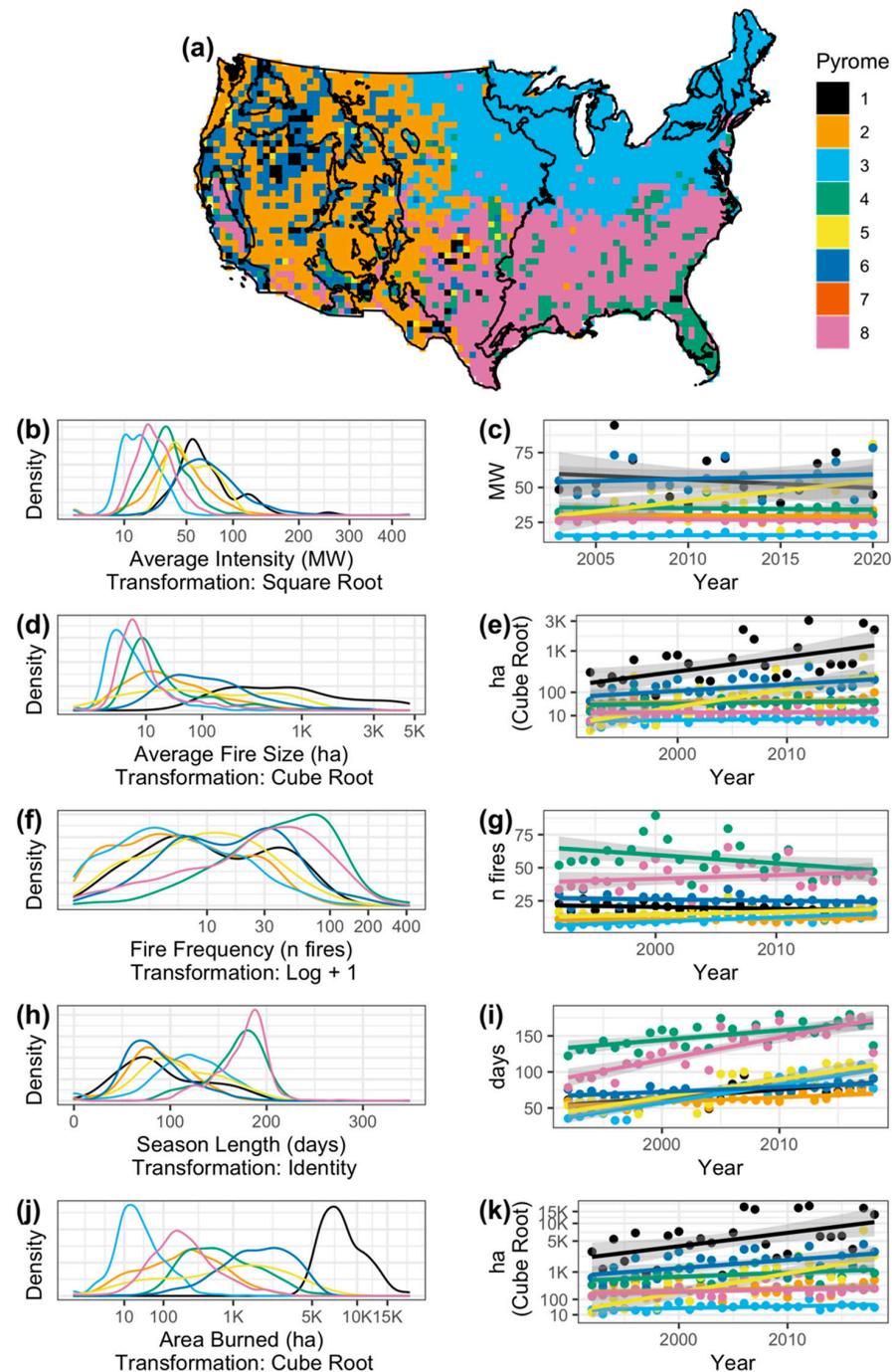
**Figure 1.** Pyrome classification scheme for *k* = 8 in the contiguous U.S. (**a**) The pyrome map with Environmental Protection Agency (EPA) Level 1 ecoregions displayed as black outlines. For each pyrome, the distributions and temporal trends are shown for the following characteristics (pyrome 7 was excluded due to insufficient sample size): (**b**,**c**) fire intensity (mean fire radiative power (FRP) from the Moderate Resolution Imaging Spectroradiometer (MODIS) in megawatts (MW)); (**d**,**e**) fire event size (mean area from the Fire Program Analysis fire-occurrence database (FPA-FOD) in hectares (ha); (**f**,**g**) frequency (number of fires from the FPA-FOD); (**h**,**i**) season length (2*sd Julian day from the FPA-FOD in days); and (**j**,**k**) burned area (sum area from the FPA-FOD in ha). All values are annual pixel means for each pyrome. For change over time, dots represent the average value for each year for each pyrome, and the trend lines (with error) were determined with linear regression. Black lines on the maps represent EPA Level 1 ecoregions.
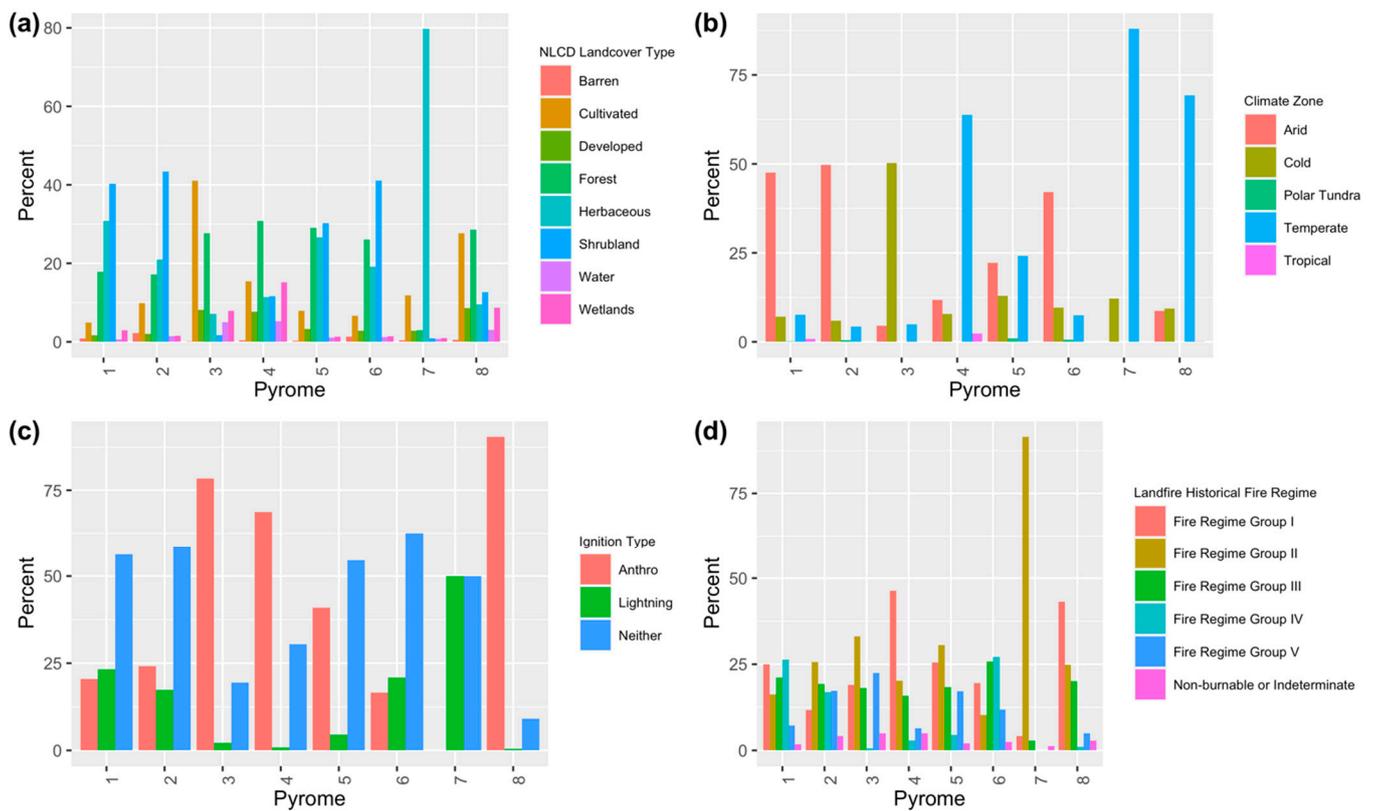
**Figure 2.** Percent of each of the eight pyromes in the contiguous U.S. occupied by each of the primary controls of fire: vegetation, climate, and ignitions: (**a**) 2016 National Land Cover Database (NLCD), (**b**) temperature- and moisture-based climate zones (Koppen–Geiger climate classification), and (**c**) ignition type, as well as (**d**) LANDFIRE historical fire regime group (FRG) category. FRG Group I: ≤35-year fire return interval, low and mixed severity; FRG Group II: ≤35-year fire return interval, replacement severity; FRG Group III: 35–200-year fire return interval, low and mixed severity; FRG Group IV: 35–200-year fire return interval, replacement severity; FRG Group V: >200-year fire return interval, any severity. A grid cell was considered dominated by anthropogenic or lightning ignitions if over 75% of ignitions in that grid cell were human or lightning-caused, respectively.

The highest average and highest extreme values for a given characteristic generally occurred in the same pyrome. For example, pyrome 5 had the highest values of mean and maximum fire size according to MTBS, and pyrome 7 did according to FPA-FOD. Although pyrome 6 had the highest values of mean FRP-based fire intensity and pyrome 1 did for maximum fire intensity, both mean and maximum values of fire intensity were not statistically different from one another between those two pyromes.

### 3.4. Constraints on Fire

Interactions between fire characteristics existed. Fire frequency generally constrained fire event size; fire event size was in the low-to-moderate range with high fire frequency and ranged more widely with lower fire frequency (Figure 3; all pairwise relationships using the same data source when possible in Figure S12). The pattern was less clear between fire frequency and FRP-based intensity, but FRP did range more widely in lower fire frequency conditions. However, these modern pyromes occupied distinct fire niche space and had unique trade-offs in fire characteristics. For example, pyromes 2 and 3 had similar mean values of fire frequency but deviated in their mean FRP-based intensity values. Similarly, pyromes 2 and 4 had similar mean FRP-based intensity values but deviated in their mean frequency values.
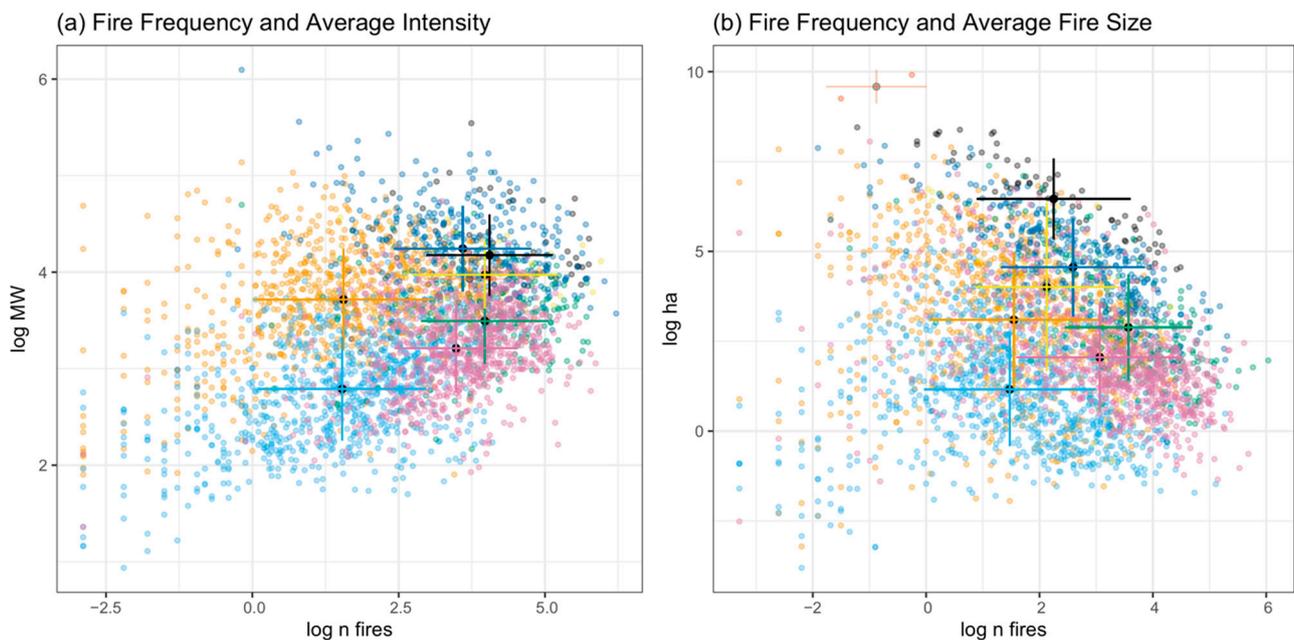
**Figure 3.** Relationships between fire physical characteristics in the contiguous U.S.: (**a**) frequency and intensity (number of fires and mean fire radiative power (FRP), megawatts (MW) from the Moderate Resolution Imaging Spectroradiometer (MODIS)) and (**b**) frequency and size (number of fires and mean fire event size, hectares (ha) from the Fire Program Analysis fire-occurrence database (FPA-FOD)). All values are log-transformed annual pixel means.

## 4. Discussion

### 4.1. Overview and Contribution to Existing Work Delineating Fire Regimes

Here, we applied a machine-learning clustering algorithm on satellite- and report-based data available on U.S. fire occurrence to evaluate the patterns of modern fires nationally, and we present a multi-scale non-nested hierarchical pyromes classification scheme. Because the clustering algorithms used to define these pyromes incorporate stochasticity, the pyromes and their perimeters are not intended to represent a definitive delineation; rather, they are intended to elucidate the core areas that share homogenous fire characteristics and general patterns of physical and anthropogenic influences on fire pyromes across the U.S. These pyromes can serve as representative groups of fire characteristics, or modern fire archetypes.

By delineating modern U.S. pyromes, or areas that share relatively homogenous fire characteristics, we expanded on previous efforts to delineate contemporary or historical fire regimes using a comprehensive suite of fire characteristics. For example, Archibald et al. [23] used five fire characteristics to define fire regimes globally; LANDFIRE fire regime groups characterize presumed historical fire regimes based on fire severity and return interval [25]; and Fire Regime Condition Class assessments identify fire regime condition classes or three classes to classify the landscape departure from reference conditions based on fire regime and vegetation characteristics [44], again using fire frequency and severity. With the work presented here, we demonstrate that variability in fire across the U.S. can be defined by an entire suite of fire characteristics, including frequency, FRP-based intensity, event size, burned area, and season length (i.e., by loading significantly onto at least one of the retained PCA components, described in Methods), which provides support for considering all these characteristics in defining modern U.S. pyromes.

### 4.2. Anthropogenic Influence on Pyromes, including Wildfire Extremes

Human ignition pressure played a large role in the East-West patterns of fire characteristics. The pyromes with human-dominated ignitions (pyromes 3, 4, and 8) in the East and

East Central U.S. had relatively moderate values of fire size, burned area, and FRP-based intensity, but some had long season lengths and fire frequency (Table S3). These pyromes dominated much of the land area of CONUS, 59% in aggregate. Conversely, pyromes characterized by relatively large and/or intense fires (pyromes 1, 5, 6, and 7) (Table S3) occupied only 14% of the CONUS land area, almost exclusively distributed across the Western and West Central U.S. and had relatively low human ignitions. Although these physically dominated pyromes were not spatially extensive, they made a disproportionate contribution to large, intense fire activity in the U.S.

Fires are becoming increasingly influenced by people over time through changing ignition pressure across CONUS. The percent of ignitions that are human-started has been increasing over time at a national scale and in all pyromes since 1992 [9] (Table S3). Further, there are indications that fire frequency and season length have also been increasing over time, but the trends are less consistent. These findings are supported by Balch et al. [8] who demonstrated expanded fire season lengths with human ignitions and by Cattau et al. [9] who demonstrated that fire season length and fire frequency are positively related to anthropogenic ignitions. Although the percent of human-started ignitions has a negative relationship with fire size, burned area, and FRP-based intensity [9] and the percent of anthropogenic ignitions has been increasing in all pyromes, fire size and total burned area have also been increasing in most pyromes. This is likely because changes in climate also affect patterns of U.S. fire activity broadly, though variably [45]. For example, it has been demonstrated extensively in the intermountain West that a strong climate signal has resulted in more frequent, larger fires of higher burn severity [10,11,46–48]. However, the extent to which climate can explain these patterns is reduced in areas that have a stronger human presence [4]. More research regarding the spatially explicit effects of human ignitions and their interactions with changing land use and climate on fire characteristics could clarify these patterns.

Furthermore, the highest average and highest extreme values for a given characteristic generally occurred in the same pyrome, indicating that spatiotemporal patterns in extreme fires are in part consistent with larger patterns of average fires. With changing modern wildfire characteristics, there has been a focus on the shift in mean values of fire parameters and, more recently, the extreme values [49,50]. While defining 'extreme' wildfire is essential [51], there is an increasing need and opportunity to explore the wealth of modern fire data to examine what are baseline fire characteristics. Such an exploration will help us to understand the full distribution of events and where extreme fires will have substantial ecological, economic, and human health impacts [52–54].

### 4.3. Fire Niche Trade-Offs

There are known trade-offs between fire characteristics that are a function of ecologically or physically driven constraints on fire processes. For example, Archibald et al. [23] found that short fire return intervals (FRIs) constrained burned area and fire intensity but that burned area and intensity are more variable at longer FRIs, likely because short FRIs do not allow sufficient time for the biomass build-up required for intense fires in some ecosystems. We found a similar pattern for fire size and FRP-based intensity as a function of fire frequency (i.e., constrained in high values of fire frequency) (Figure 3). We expanded on these concepts by demonstrating how these trade-offs varied by pyrome and how they were moderated by vegetation type, climate, and ignition type. For example, the pyromes positioned in the lower range of FRP-based fire intensity and size for their fire frequency values (pyromes 3, 4, and 8) were dominated by forest and/or cultivated land-cover types, temperate or cold climates, and more human ignitions; pyromes with higher FRP-based intensity and size with respect to fire frequency (pyromes 1, 2, and 6) were dominated by shrubland and/or herbaceous land-cover types with arid and/or cold climates and had fewer human ignitions. The biophysical characteristics of forest and of temperate climates may make these areas less amenable to large, intense fires with a given fire frequency than shrubland and herbaceous areas in arid climates. Further, areas with cultivated land and

many human ignitions are associated with higher human population density in general and likely have a greater capacity for human intervention which may result in reduced fire size and FRP-based intensity despite the likely increases in fire frequency.

### 4.4. Controls on Fire

Each pyrome consisted of a relatively heterogeneous mix of the controls on fire (i.e., vegetation type, climate zone, or ignition source), though patterns with climate were more pronounced. In every pyrome except one (pyrome 7) which was limited in spatial extent, the NLCD dominant coarse vegetation type occupied less than 65% of the pyrome. Although three pyromes were clearly dominated by human ignitions, the others were more mixed in terms of ignition type. However, pyromes were more climatologically homogeneous; the dominant coarse climate category for each pyrome represented over 50% of that pyrome, reinforcing the consensus in the literature of the strong influence of climate on modern, broad-scale fire processes [10,11,46–48]. Because each pyrome was heterogeneous in terms of vegetation, and ignition type, and somewhat with climate, further work exploring how trade-offs in fire characteristics vary as a function of each of those variables across broad spatial scales independent of the pyrome framework would elucidate the mechanisms behind the trends demonstrated here. It may be challenging to predict future changes in fire regimes as a function of these variables, as the pathways of change may vary [23].

### 4.5. Relationship with Ecoregions and FRGs and Relevance to Historical Context

A spatial mismatch between our derived modern pyromes and both ecoregions (Figure 1a) and historical fire regimes (Figure 2d) suggests that vegetation-based classification systems may be limited in their ability to fully explain modern U.S. fire patterns. As mentioned in the Introduction, we used the term 'pyrome' rather than 'fire regime' when exploring how human ignitions shape our modern fire characteristics, because we used contemporary fire data from an approximately 40-year period to derive these clusters that share similar values of fire characteristics. In a historical context, 40 years is a short time period, a relatively static moment in a changing, dynamic system. Although we incorporated many of the characteristics often used to define fire regimes in our pyromes (e.g., frequency, size), a direct comparison between historical fire regimes and modern pyromes—and defining modern fire regimes more generally—is complicated by the uncertainty in these dynamics. Meaning, the patterns we detected during this snapshot may truly represent longer-term trends, or they may essentially be interpreted as noise from a long-term perspective [18,24].

Current fire characteristics are undoubtedly influenced by the historical legacies, as well as current patterns of human activity across U.S. landscapes. The anthropogenic 'wave of fire' describes the human signal on fire regimes in the U.S., or changes in fire characteristics over broad spatial scales as a function of changing human activity [55]. Fire was extensively used as a management tool by indigenous people before European colonization. Human-caused ignitions declined during industrialization, with even steeper declines during the fire exclusion era in the 20th century [3,55–57]. The more recent adoption of prescribed burning and let-it-burn policies may reflect the growing perception of fire as integral to the landscape [53]; however, the majority of U.S. fires are still suppressed [58].

This 'wave of fire' [55], or changes in anthropogenic fire over broad spatial scales, would affect fire characteristics, such as fire frequency and fire return intervals. Although substantial evidence exists for this historical pattern of human ignitions across the U.S., the extent to which it is broadly geographically applicable is unknown, which could affect our interpretation of the magnitude of the influence of modern human ignitions on fire characteristics in a historical context. Further, the influence of people on fire processes has varied over space and time with changing and complex interactions between ignitions, biomass, and climate. For example, in the mountain big sagebrush biome, modern changes in fire characteristics are attributed to changes in ignition patterns and fuel characteristics during the mid-1800s with European settlement, as well as the interaction of many factors in modern times, including land development for agriculture and human habitation, the

distributional shifts of other vegetation (e.g., invasive grasses and woodland expansion), fire exclusion, and climate change [59]. We cannot dismiss the importance of either historical or modern human activity in shaping contemporary fire characteristics. The analysis of the spatial overlap between modern pyromes and LANDFIRE historical fire regimes is intended to frame the contemporary fire patterns described in this paper within a historical context, rather than to elucidate change from historical times, as the fire characteristics we used in the pyromes classification are not consistent with those used to derive LANDFIRE historical fire regimes. As a general pattern, our modern pyromes were heterogeneously distributed in the Western U.S., which is consistent with the patterns seen in the historical fire regimes.

*4.6. Relevance to Management across Scales*

In this work, we aimed to delineate the areas that share relatively homogeneous fire characteristics to identify areas in which contemporary fire was most similar. This work can be used to inform fire management, as pyromes delineated based on fire physical characteristics build a framework in which the units of evaluation are as internally homogeneous as possible across multiple variables. The delineation of pyromes at different scales of aggregation allows for the complexity of the classification to be adjusted to levels appropriate for a variety of purposes, including examining how fire characteristics are changing in a given area under climate and land-use changes. We do not suggest that we manage at the scale of the $k = 8$ pyrome classification, as there is great variation in how extensive and spatially clustered each pyrome is. However, finer levels of aggregation could be more useful at the state or regional level (Figure S11), particularly when informed by the variety of environmental and social complexities relevant to management and restoration goals at various scales. These relevant variables, including ignition type, are not incorporated into the delineation of pyromes themselves in order to preserve the possibility of assessing patterns of fire characteristics *sensu stricto*. These relevant variables could then be incorporated in additional analyses to capture a fuller picture of fire patterns *sensu lato*. Being able to differentiate between local, regional, and sub-continental patterns enables the perspective of zones of human impact.

*4.7. Caveats on Data and Scale of Analyses*

The choice of which fire data were used in the analyses influenced the results. Although patterns in fire characteristics were often consistent among the fire datasets (Table S3), this was not always the case (see additional text to this point in Results). Because of the unique properties of each dataset, fire characteristics generated by each dataset would offer different and complementary information on fires. For example, because the MTBS product has a minimum size threshold, some fires are included in the other datasets that might be excluded in the MTBS data. This issue would affect both fire characteristics and trends over time derived from MTBS. Simply igniting a fire versus growing that fire to the MTBS size threshold depends on different climatic and fuel drivers, and therefore trends and statistics derived from these datasets are likely signaling different components of fire processes. We used the FPA-FOD dataset for trend analyses (Figure 1) for the reasons noted in the Methods section; however, differences in reporting among states and over time could affect these results. A comprehensive view of spatiotemporal fire patterns would consider the suite of variables derived from multiple datasets.

Similarly, there are a number of additional national-scale fire products that were not included in this analysis (e.g., MODIS Burned Area MDC64A1.006 [60]; Landsat Burned Area [61,62]; Combined wildland fire dataset [63]) that may capture fire characteristics that the datasets we used do not capture. A fire product that aggregates various fire products, including those used in this paper, while retaining the information in each would push forward our understanding of fire processes across large scales. Due to the extensive data integration challenges of such an effort, creating this product is outside the scope of this study. This issue of not incorporating all fire datasets may be particularly relevant for fires

in cropland areas, which are not included in the MTBS or FPA-FOD datasets and are known to have high omission areas in other datasets due to their smaller size, shorter duration, and/or lower intensity values [64]. The majority of the land area classified as cultivated land by the NLCD dataset was grouped into pyrome 3 (51%) and pyrome 8 (30%), both of which are dominated by human ignitions and have moderate values for event size, burned area, and intensity [65]. This grouping is consistent with what we might expect for cropland fires given their characteristics, though the omission of cropland fires certainly influenced our pyromes clustering and our analyses of characteristics and trends. Cropland fires may be better captured by burned area products derived from moderate-resolution satellites [64], and an analysis using that dataset could increase our understanding of how cropland fires contribute to spatiotemporal patterns of fire activity.

We focused on the classification with eight pyromes. Although the established cut points of $k$ were derived from thorough statistical analysis, the choice of which level to use to make these comparisons likely influenced the results and conclusions. For example, a smaller number $k$ would likely increase heterogeneity within each pyrome, and larger numbers of $k$ would become increasingly difficult to interpret. We evaluated the relationships of the pyromes to one another at different scales (Figures S10 and S11) but did not conduct a complete multiscalar analysis. Further, we chose an annual, 50 km resolution for the analysis, which also had implications for the results and conclusions. For example, 2810 MTBS fire events, representing ~9.6% of the fires in that dataset, were larger than 50 km$^2$. Values associated with these fires were assigned to the grid cell in which the fire centroid occurred, and thus this approach did not capture the full spatial influence of very large fires. At coarser spatial resolutions, individual large fire events would be more likely to fall within a single grid cell; however, heterogeneity in fire characteristics captured at the 50 km resolution would be lost. As another example, the temporal resolution of our analysis allowed us to track annual trends in fire activity over time; however, a finer temporal resolution might reveal relevant intra-annual patterns in fire characteristics that are obscured at the annual resolution. A multiscalar analysis evaluating a range of pyrome aggregations derived from data compiled across a variety of spatiotemporal resolutions could shed light on how modern pyromes track onto spatial patterns of variables such as climate, vegetation, and ecotypes across scales and could elucidate different patterns of change. For example, a spatiotemporally explicit evaluation of the relationship between fire characteristics with fuels (e.g., the LANDFIRE project's spatial fuel datasets), human population density (e.g., CIESIN) [66], and climate (e.g., WorldClim historical monthly weather data) [67] would contribute to a mechanistic understanding of contemporary fire patterns.

## 5. Conclusions

Here, in using machine learning to delineate modern pyromes in the U.S. at different scales of aggregation, we demonstrated that previous efforts to detail fire regimes can be complemented by considering a data-driven approach that uses a suite of fire characteristics related to fire frequency, fire event size, total burned area, FRP-based fire intensity, and season length. We found that approximately 59% of CONUS, primarily in the East and East Central U.S., was represented by pyromes dominated by human ignitions, and these areas exhibit moderate fire sizes, intensities, and total burned area. Pyromes with the largest fire sizes, highest intensities, or greatest total burned area represented only 14% of the U.S., primarily in the West and West Central U.S., and these areas had a relatively low percent of ignitions that were human-started. However, fires are becoming increasingly influenced by people over time across CONUS, as the percent of pixels that are dominated by human ignitions has been increasing over time in all modern pyromes (Table S3). Furthermore, there are known trade-offs between fire characteristics that are a function of ecologically or physically driven constraints on fire processes, and these trade-offs for contemporary fires are affected by vegetation type, climate, and ignition type. We conclude that modern pyromes, which are relatively internally homogeneous in their fire characteristics, serve

as an appropriate spatial framework for research on fire processes and can contribute to fire management decisions. Akin to delineating ecoregions or climate zones this work established a framework for understanding modern U.S. fire patterns and how they are changing nationally by providing fundamental, consistent units of fire zones.

## Appendix A. Description of the Pyromes (*k* = 8)

We report any class that constituted at least 20% of a given pyrome for each category.

Pyrome 1: Extreme, intense fires in the West. This pyrome has the highest value for maximum intensity and is not significantly different from the pyrome with the highest value for mean intensity (pyrome 6). It constitutes only ~2% of the area of CONUS. It is a spatially disaggregated pyrome distributed primarily throughout North American Deserts (44% of the pyrome is located in that Ecoregion) and the Northwestern Forested

Mountains (23%), primarily arid climate zones (61%) on shrubland (40%) and herbaceous (31%) land-cover types. Fire history was mixed in this area with low- and mixed-severity fires ($\leq$35-year fire return interval (FRI) in LANDFIRE fire regime group (FRG) I and 35–200 FRI in FRG III, 25% and 21%, respectively), as well as replacement-severity fires with a 35–200 FRI in FRG IV, 26%). The anthropogenic influence on ignitions is relatively low; approximately half of the pyrome is dominated by anthropogenic fires (Table S3), and only 21% of the mean annual fires are anthropogenic (Table S4).

Pyrome 2: Moderate fire characteristics in the West and Central U.S. This pyrome does not have the highest values for any of the fire characteristics assessed. This pyrome occurs in mostly arid (71%) and cold (21%) climates on shrubland (43%) and herbaceous (21%) land-cover types. This pyrome occupies ~27% of CONUS, and it occurs primarily in the North American Deserts (42%) and the Great Plains (30%). Fire history is quite mixed in this area; the only FRG that represents >20% in this area is FRG Group II with $\leq$35-year FRI and replacement severity. Similar to pyrome 1, the anthropogenic influence on ignitions is relatively low; approximately half of the pyrome is dominated by anthropogenic fires, and only 24% of the mean annual fires are anthropogenic.

Pyrome 3: Moderate, human-started fires in the Northeast and North Central U.S. This pyrome has the highest value for the proportion of pixels dominated by anthropogenic ignitions (90% of the pyrome area is dominated by anthropogenic fires), and 78% of the mean annual fires are anthropogenic. It also has the highest rate of increase in anthropogenic fires over time. This pyrome occupies ~28% of CONUS, primarily in the Northeastern US: the Eastern Temperate Forests (49%) and the Great Plains (31%) in mostly cold climates (89%) on cultivated land (41%) and forest (28%). This pyrome has quite mixed fire history, with $\leq$35-year FRI with replacement severity (FRG II, 33%) or >200-year FRI of any severity (FRG V, 23%). It also has the fastest rate of increase in fire frequency according to the FPA-FOD.

Pyrome 4: Frequent, human-started fires with long season lengths in the Southeast and South Central U.S. This pyrome has the most frequent fire of all pyromes according to MTBS and FPA-FOD and is not significantly different from the pyrome with the most frequent fire according to MODIS (Pyrome 5). The rate of increase for fire frequency is also greatest in this pyrome according to MTBS. It also has the longest season length and greatest rate of increase according to MTBS and MODIS, respectively. Along with pyrome 3, this pyrome has a relatively high human influence; 80% of the pyrome area is dominated by anthropogenic fires, and 69% of the mean annual fires are anthropogenic. It occupies just 7% of CONUS, is relatively disaggregated, and is located in the Southeastern U.S., as well as scattered Westward from that area. Eastern Temperate Forests (62%) and the Great Plains (22%) in mostly temperate climates (67%). It is dominated by forest (31%), with no other land-cover type representing $\geq$20% of the pyrome. Historically, these areas had $\leq$35-year FRI with either low and mixed severity (FRG I, 46%) or replacement severity (FRG II, 20%).

Pyrome 5: Frequent, extreme large fires with increasing intensity disaggregated across the Central and Western U.S. This pyrome has the highest value of fire frequency and rate of increase according to MODIS (and is not significantly different from the pyrome with the fastest rate of increase in frequency according to FPA-FOD). It also has the highest value of maximum (i.e., extreme) fire size and burned area, the fastest rate of increase for those variables, and the highest value of mean fire size according to MTBS. There is evidence that intensity is increasing here as well; it has the fastest rate of increase in maximum intensity and is not significantly different from the pyrome with the fastest rate of increase in mean intensity. The anthropogenic influence on ignitions is moderate; 60% of the pyrome is dominated by anthropogenic fires, and 41% of the mean annual fires are anthropogenic. It occupies only <1% of CONUS and is disaggregated across the Central and Western U.S. in the Great Plains (36%), and Northwestern Forested Mountains (36%). It occurs on forest (20%), shrubland (30%), and herbaceous (27%) land-cover types in temperate (43%), arid (28%), and cold (28%) climates. Similar to pyrome 4, historically, these areas had $\leq$35-year FRI with either low and mixed severity (FRG I, 26%) or replacement severity (FRG II, 31%).

Pyrome 6: Intense fires in the West. This pyrome has the highest value for mean intensity and is not significantly different from the pyrome with the highest value for maximum intensity (pyrome 1). It occupies ~11% of CONUS and occurs primarily in the Western US: Northwestern Forested Mountains (39%) and North American Deserts (35%), in mostly arid (55%) and cold (30%) climates on shrubland (41%) and forest (26%) land-cover types. Historically, fires had 35–200-year FRIs with either low and mixed severity (FRG III, 26%) or replacement severity (FRG IV, 27%). Similar to pyrome 1, the anthropogenic influence on ignitions is relatively low; approximately half of the pyrome is dominated by anthropogenic fires, and only 17% of the mean annual fires are anthropogenic.

Pyrome 7: Large and extreme large lightning fires concentrated in the Great Plains. This pyrome is characterized by large fires, with some evidence of high intensity, frequency, and season lengths. For fire size, it has the highest values for mean fire size, maximum fire size, and burned area, as well as rates of increase for those variables, according to FPAA-FOD; it also has the maximum rate of increase for maximum fire size according to MTBS and was not significantly different from the maximum rate of increase for mean fire size according to MTBS. It is also not significantly different from the pyrome with the highest value for fire frequency and rate of increase, according to some datasets, nor is it significantly different from the pyrome with the highest value for mean and maximum intensity; it also has the fastest rate of increase for mean intensity. It is significantly different from the pyrome with the highest value for season length or rate of increase according to some datasets. It occupies only <1% of CONUS and is concentrated exclusively in the Great Plains (100%) in temperate (88%) climates, primarily in herbaceous (80%) areas. Fire history here is almost exclusively ≤35-year FRIs with replacement severity (FRG II, 92%). Similar to pyromes 1 and 2, the anthropogenic influence on fire ignitions is low; 30% of the pyrome is dominated by anthropogenic fires, and 0% of the mean annual fires are anthropogenic. It has the highest value for lightning fires (50%).

Pyrome 8: Human-started fires with long season lengths in the Southeast and South Central U.S. This pyrome has moderate fire characteristics over long season lengths. It has the longest season length according to MODIS and FPA-FOD and the highest rate of increase according to FPA-FOD. This pyrome occupies ~24% of CONUS. It is located primarily in the Southeastern US—Eastern Temperate Forests (63%) and the Great Plains (29%)—and is composed of forest and cultivated land-use/land-cover types (29% and 28%, respectively) in mostly temperate climates (71%). Historically, these areas had ≤35-year FRI with either low and mixed severity (FRG I, 43%) or replacement severity (FRG II, 25%) or 35–200-year FRIs with low and mixed severity (FRG III, 20%). Similar to pyrome 3, this pyrome is dominated by human ignitions; 90% of the pyrome area is dominated by anthropogenic fires. 90% of the mean annual fires are anthropogenic, the highest value among the pyromes.

## References

1. Krawchuk, M.A.; Moritz, M.A.; Parisien, M.-A.; Van Dorn, J.; Hayhoe, K. Global pyrogeography: The current and future distribution of wildfire. *PLoS ONE* **2009**, *4*, e5102. [CrossRef] [PubMed]
2. Daniau, A.; Bartlein, P.J.; Harrison, S.P.; Prentice, I.C.; Brewer, S.; Friedlingstein, P.; Harrison-Prentice, T.I.; Inoue, J.; Izumi, K.; Marlon, J.R.; et al. Predictability of biomass burning in response to climate changes. *Glob. Biogeochem. Cycles* **2012**, *26*, 4249. [CrossRef]
3. Taylor, A.H.; Trouet, V.; Skinner, C.N.; Stephens, S. Socioecological transitions trigger fire regime shifts and modulate fire–climate interactions in the Sierra Nevada, USA, 1600–2015 CE. *Proc. Natl. Acad. Sci. USA* **2016**, *113*, 13684–13689. [CrossRef] [PubMed]
4. Syphard, A.D.; Keeley, J.E.; Pfaff, A.H.; Ferschweiler, K. Human presence diminishes the importance of climate in driving fire activity across the United States. *Proc. Natl. Acad. Sci. USA* **2017**, *114*, 13750–13755. [CrossRef] [PubMed]
5. Higuera, P.E.; Abatzoglou, J.; Littell, J.S.; Morgan, P. The changing strength and nature of fire-climate relationships in the Northern Rocky Mountains, USA, 1902–2008. *PLoS ONE* **2015**, *10*, e0127563. [CrossRef]
6. Fréjaville, T.; Curt, T. Seasonal changes in the human alteration of fire regimes beyond the climate forcing. *Environ. Res. Lett.* **2017**, *12*, 035006. [CrossRef]
7. Abatzoglou, J.T.; Williams, A.P. Impact of anthropogenic climate change on wildfire across western US forests. *Proc. Natl. Acad. Sci. USA* **2016**, *113*, 11770–11775. [CrossRef]

8.  Balch, J.K.; Bradley, B.A.; Abatzoglou, J.T.; Nagy, R.C.; Fusco, E.J.; Mahood, A.L. Human-started wildfires expand the fire niche across the United States. *Proc. Natl. Acad. Sci. USA* **2017**, *114*, 2946–2951. [CrossRef]
9.  Cattau, M.E.; Wessman, C.; Mahood, A.; Balch, J.K. Anthropogenic and lightning-started fires are becoming larger and more frequent over a longer season length in the U.S.A. *Glob. Ecol. Biogeogr.* **2020**, *29*, 668–681. [CrossRef]
10. Dennison, P.E.; Brewer, S.C.; Arnold, J.D.; Moritz, M.A. Large wildfire trends in the western United States, 1984–2011. *Geophys. Res. Lett.* **2014**, *41*, 2928–2933. [CrossRef]
11. Westerling, A.L.; Hidalgo, H.G.; Cayan, D.R.; Swetnam, T.W. Warming and earlier spring increase western U.S. forest wildfire activity. *Science* **2006**, *313*, 940–943. [CrossRef]
12. Williams, A.P.; Abatzoglou, J.T.; Gershunov, A.; Guzman-Morales, J.; Bishop, D.A.; Balch, J.K.; Lettenmaier, D.P. Observed impacts of anthropogenic climate change on wildfire in California. *Earth's Future* **2019**, *7*, 892–910. [CrossRef]
13. Parisien, M.-A.; Miller, C.; Parks, S.A.; DeLancey, E.R.; Robinne, F.-N.; Flannigan, M.D. The spatially varying influence of humans on fire probability in North America. *Environ. Res. Lett.* **2016**, *11*, 75005. [CrossRef]
14. Radeloff, V.C.; Helmers, D.P.; Kramer, H.A.; Mockrin, M.H.; Alexandre, P.M.; Bar-Massada, A.; Butsic, V.; Hawbaker, T.J.; Martinuzzi, S.; Syphard, A.D.; et al. Rapid growth of the US wildland-urban interface raises wildfire risk. *Proc. Natl. Acad. Sci. USA* **2018**, *115*, 3314–3319. [CrossRef] [PubMed]
15. Bond, W.J.; Keeley, J.E. Fire as a global 'herbivore': The ecology and evolution of flammable ecosystems. *Trends Ecol. Evol.* **2005**, *20*, 387–394. [CrossRef] [PubMed]
16. Krebs, P.; Pezzatti, G.B.; Mazzoleni, S.; Talbot, L.M.; Conedera, M. Fire regime: History and definition of a key concept in disturbance ecology. *Theory Biosci.* **2010**, *129*, 53–69. [CrossRef]
17. Morgan, P.; Hardy, C.C.; Swetnam, T.W.; Rollins, M.G.; Long, D.G. Mapping fire regimes across time and space: Understanding coarse and fine-scale fire patterns. *Int. J. Wildland Fire* **2001**, *10*, 329–342. [CrossRef]
18. Keane, R. Disturbance regimes and the historical range and variation in terrestrial ecosystems. *Ref. Modul. Life Sci.* **2017**, *2*, 568–581. [CrossRef]
19. Flannigan, M.; Haar, T.V. Forest fire monitoring using NOAA satellite AVHRR. *Can. J. For. Res.* **1986**, *16*, 975–982. [CrossRef]
20. Hawbaker, T.; Radeloff, V.C.; Stewart, S.I.; Hammer, R.B.; Keuler, N.S.; Clayton, M.K. Human and biophysical influences on fire occurrence in the United States. *Ecol. Appl.* **2013**, *23*, 565–582. [CrossRef]
21. Short, K.C. *Spatial Wildfire Occurrence Data for the United States, 1992–2013*; Forest Service Research Data Archive: Fort Collins, CO, USA, 2017.
22. Nagy, R.C.; Fusco, E.J.; Bradley, B.A.; Abatzoglou, J.T.; Balch, J.K. Human-related ignitions increase the number of large wildfires across U.S. ecoregions. *Fire* **2018**, *1*, 4. [CrossRef]
23. Archibald, S.; Lehmann, C.E.R.; Gómez-Dans, J.L.; Bradstock, R.A. Defining pyromes and global syndromes of fire regimes. *Proc. Natl. Acad. Sci. USA* **2013**, *110*, 6442–6447. [CrossRef] [PubMed]
24. Whitlock, C.; Higuera, P.E.; McWethy, D.B.; Briles, C.E. Paleoecological perspectives on fire ecology: Revisiting the fire-regime concept. *Open Ecol. J.* **2010**, *3*, 6–23. [CrossRef]
25. Rollins, M.G. LANDFIRE: A nationally consistent vegetation, wildland fire, and fuel assessment. *Int. J. Wildland Fire* **2009**, *18*, 235–249. [CrossRef]
26. Giglio, L.; Descloitres, J.; Justice, C.O.; Kaufman, Y.J. An enhanced contextual fire detection algorithm for MODIS. *Remote Sens. Environ.* **2003**, *87*, 273–282. [CrossRef]
27. Eidenshink, J.; Schwind, B.; Brewer, K.; Zhu, Z.-L.; Quayle, B.; Howard, S. A Project for monitoring trends in burn severity. *Fire Ecol.* **2007**, *3*, 3–21. [CrossRef]
28. Short, K.C. *Spatial Wildfire Occurrence Data for the United States, 1992–2018*, 5th ed.; [FPA_FOD_20210617]; Forest Service Research Data Archive: Fort Collins, CO, USA, 2021. [CrossRef]
29. Schroeder, W.; Csiszar, I.; Giglio, L.; Schmidt, C.C. On the use of fire radiative power, area, and temperature estimates to characterize biomass burning via moderate to coarse spatial resolution remote sensing data in the Brazilian Amazon. *J. Geophys. Res. Earth Surf.* **2010**, *115*, 3769. [CrossRef]
30. Rossi, J.L.; Chatelon, F.J.; Marcelli, T. Fire Intensity. In *Encyclopedia of Wildfires and Wildland-Urban Interface (WUI) Fires*; Manzello, S., Ed.; Springer: Cham, Switzerland, 2019.
31. Wooster, M.J.; Roberts, G.; Perry, G.; Kaufman, Y.J. Retrieval of biomass combustion rates and totals from fire radiative power observations: FRP derivation and calibration relationships between biomass consumption and fire radiative energy release. *J. Geophys. Res. Earth Surf.* **2005**, *110*, 6318. [CrossRef]
32. Giglio, L.; Csiszar, I.; Restás, Á.; Morisette, J.T.; Schroeder, W.; Morton, D.; Justice, C.O. Active fire detection and characterization with the advanced spaceborne thermal emission and reflection radiometer (ASTER). *Remote Sens. Environ.* **2008**, *112*, 3055–3063. [CrossRef]
33. Freeborn, P.H.; Wooster, M.J.; Roy, D.P.; Cochrane, M.A. Quantification of MODIS fire radiative power (FRP) measurement uncertainty for use in satellite-based active fire characterization and biomass burning estimation. *Geophys. Res. Lett.* **2014**, *41*, 1988–1994. [CrossRef]
34. R Core Team. *R: A Language and Environment for Statistical Computing*; R Core Team: Vienna, Austria, 2022. Available online: https://www.R-project.org/ (accessed on 3 July 2022).

35. Kassambara, A.; Fabian, M. Factoextra: Extract and Visualize the Results of Multivariate Data Analyses. 2019. Available online: https://CRAN.R-project.org/package=factoextra (accessed on 3 July 2022).

36. Brock, G.; Pihur, V.; Datta, S.; Datta, S. clValid: An R package for cluster validation. *J. Stat. Softw.* **2008**, *25*, 1–22. [CrossRef]

37. Pinheiro, J.; Bates, D.; DebRoy, S.; Sarkar, D. *Nlme: Linear and Nonlinear Mixed Effects Models*; R Core Team: Vienna, Austria, 2013.

38. Jin, S.; Homer, C.; Yang, L.; Danielson, P.; Dewitz, J.; Li, C.; Zhu, Z.; Xian, G.; Howard, D. Overall methodology design for the United States National land cover database 2016 products. *Remote Sens.* **2019**, *11*, 2971. [CrossRef]

39. Kottek, M.; Grieser, J.; Beck, C.; Rudolf, B.; Rubel, F. World map of the Köppen-Geiger climate classification updated. *Meteorol. Z.* **2006**, *15*, 259–263. [CrossRef]

40. Omernik, J.M. Ecoregions of the conterminous United States. *Ann. Assoc. Am. Geogr.* **1987**, *77*, 118–125. [CrossRef]

41. Omernik, J.M. Ecoregions: A Spatial Framework for Environmental Management. In *Biological Assessment and Criteria: Tools for Water Resource Planning and Decision Making*; Davis, W.S., Simon, T.P., Eds.; Lewis Publishers: Boca Raton, FL, USA, 1995; pp. 49–62.

42. Omernik, J.M. Perspectives on the Nature and Definition of Ecological Regions. *Environ. Manag.* **2004**, *34*, S27–S38. [CrossRef]

43. Omernik, J.M.; Griffith, G.E. Ecoregions of the conterminous united states: Evolution of a hierarchical spatial framework. *Environ. Manag.* **2014**, *54*, 1249–1266. [CrossRef]

44. Hann, W.J.; Shlisky, A.; Havlina, D.; Schon, K.; Barrett, S.W.; DeMeo, T.E.; Pohl, K.; Menakis, J.P.; Hamilton, D.; Jones, J.; et al. *Interagency Fire Regime Condition Class Guidebook*; Homepage of the Interagency Fire Regime Condition Class Website; USDA Forest Service, US Department of the Interior, The Nature Conservancy: Boise, ID, USA, 2010.

45. Morton, D.C.; Collatz, G.J.; Wang, D.; Randerson, J.T.; Giglio, L.; Chen, Y. Satellite-based assessment of climate controls on US burned area. *Biogeosciences* **2013**, *10*, 247–260. [CrossRef]

46. Balch, J.K.; Schoennagel, T.; Williams, A.P.; Abatzoglou, J.T.; Cattau, M.E.; Mietkiewicz, N.P.; Denis, L.A.S. Switching on the Big Burn of 2017. *Fire* **2018**, *1*, 17. [CrossRef]

47. Dillon, G.K.; Holden, Z.A.; Morgan, P.; Crimmins, M.A.; Heyerdahl, E.K.; Luce, C.H. Both topography and climate affected forest and woodland burn severity in two regions of the western US, 1984 to 2006. *Ecosphere* **2011**, *2*, art130–art133. [CrossRef]

48. Westerling, A.L. Increasing western US forest wildfire activity: Sensitivity to changes in the timing of spring. *Philos. Trans. R. Soc. B Biol. Sci.* **2016**, *371*, 20150178. [CrossRef]

49. Joseph, M.B.; Rossi, M.W.; Mietkiewicz, N.P.; Mahood, A.L.; Cattau, M.E.; Denis, L.A.S.; Nagy, R.C.; Iglesias, V.; Abatzoglou, J.T.; Balch, J.K. Spatiotemporal prediction of wildfire size extremes with Bayesian finite sample maxima. *Ecol. Appl.* **2019**, *29*, e01898. [CrossRef]

50. Williams, J. Exploring the onset of high-impact mega-fires through a forest land management prism. *For. Ecol. Manag.* **2013**, *294*, 4–10. [CrossRef]

51. Tedim, F.; Leone, V.; Amraoui, M.; Bouillon, C.; Coughlan, M.R.; Delogu, G.M.; Fernandes, P.M.; Ferreira, C.; McCaffrey, S.; McGee, T.K.; et al. Defining extreme wildfire events: Difficulties, challenges, and impacts. *Fire* **2018**, *1*, 9. [CrossRef]

52. Kochi, I.; Donovan, G.H.; Champ, P.A.; Loomis, J.B. The economic cost of adverse health effects from wildfire-smoke exposure: A review. *Int. J. Wildland Fire* **2010**, *19*, 803–817. [CrossRef]

53. McCaffrey, S.; Toman, E.; Stidham, M.; Shindler, B. Social science research related to wildfire management: An overview of recent findings and future research needs. *Int. J. Wildland Fire* **2013**, *22*, 15–24. [CrossRef]

54. Thompson, D.M.P.; Calkin, D.E.; Finney, M.A.; Ager, A.A.; Gilbertson-Day, J.W. Integrated national-scale assessment of wildfire risk to human and ecological values. *Stoch. Hydrol. Hydraul.* **2011**, *25*, 761–780. [CrossRef]

55. Stambaugh, M.C.; Marschall, J.M.; Abadir, E.R.; Jones, B.C.; Brose, P.H.; Dey, D.C.; Guyette, R.P. Wave of fire: An anthropogenic signal in historical fire regimes across central Pennsylvania, USA. *Ecosphere* **2018**, *9*, e02222. [CrossRef]

56. Van Lear, D.H.; Harlow, R.F. *Fire in the Eastern United States: Influence on Wildlife Habitat*; Gen. Tech. Rep. NE-288; U.S. Department of Agriculture, Forest Service, Northeastern Research Station: Newtown Square, PA, USA, 2002.

57. Pyne, S.J. America's fires: A historical context for policy and practice. *Technol. Cult.* **2011**, *52*, 646–647.

58. North, M.P.; Stephens, S.L.; Collins, B.M.; Agee, J.K.; Aplet, G.; Franklin, J.F.; Fule, P.Z. Reform forest fire management. *Science* **2015**, *349*, 1280–1281. [CrossRef]

59. Innes, R.J.; Zouhar, K. *Fire Regimes of Mountain Big Sagebrush Communities*; U.S. Department of Agriculture, Forest Service, Rocky Mountain Research Station, Missoula Fire Sciences Laboratory: Missoula, MT, USA, 2018. Available online: https://www.fs.fed.us/database/feis/fire_regimes/mountain_big_sagebrush/all.html (accessed on 15 May 2020).

60. Giglio, L.; Boschetti, L.; Roy, D.P.; Humber, M.L.; Justice, C.O. The Collection 6 MODIS burned area mapping algorithm and product. *Remote Sens. Environ.* **2018**, *217*, 72–85. [CrossRef]

61. Hawbaker, T.J.; Vanderhoof, M.K.; Beal, Y.-J.; Takacs, J.D.; Schmidt, G.L.; Falgout, J.T.; Williams, B.; Fairaux, N.M.; Caldwell, M.K.; Picotte, J.J.; et al. Mapping burned areas using dense time-series of Landsat data. *Remote Sens. Environ.* **2017**, *198*, 504–522. [CrossRef]

62. Hawbaker, T.J.; Vanderhoof, M.K.; Schmidt, G.L.; Beal, Y.-J.; Picotte, J.J.; Takacs, J.D.; Falgout, J.T.; Dwyer, J.L. The Landsat Burned Area algorithm and products for the conterminous United States. *Remote Sens. Environ.* **2020**, *244*, 111801. [CrossRef]

63. Welty, J.L.; Jeffries, M.I. Combined wildland fire datasets for the United States and certain territories, 1800s-Present: U.S. Geological Survey data release. 2021. [CrossRef]

64. Hall, J.V.; Loboda, T.V.; Giglio, L.; McCarty, G.W. A MODIS-based burned area assessment for Russian croplands: Mapping requirements and challenges. *Remote Sens. Environ.* **2016**, *184*, 506–521. [CrossRef]

65. Hall, J.V.; Argueta, F.; Giglio, L. Validation of MCD64A1 and FireCCI51 cropland burned area mapping in Ukraine. *Int. J. Appl. Earth Obs. Geoinformation ITC J.* **2021**, *102*, 102443. [CrossRef]

66. Center for International Earth Science Information Network—CIESIN—Columbia University. *Gridded Population of the World, Version 4 (GPWv4): Population Density, Revision 11*; NASA Socioeconomic Data and Applications Center (SEDAC): Palisades, NY, USA, 2018. [CrossRef]

67. Fick, S.E.; Hijmans, R.J. WorldClim 2: New 1-km spatial resolution climate surfaces for global land areas. *Int. J. Climatol.* **2017**, *37*, 4302–4315. [CrossRef]